1-1-2013

Time-of-flight polarized neutron reflectometry on PLATYPUS: status and future developments

T Saerbeck
ANSTO

D L. Cortie
University of Wollongong, dlc422@uowmail.edu.au

S Bruck
ANSTO

J Bertinshaw
ANSTO

S A. Holt
ANSTO

See next page for additional authors

Time-of-flight polarized neutron reflectometry on PLATYPUS: status and future developments

Abstract

Time-of-flight (ToF) polarized neutron reflectometry enables the detailed investigation of depth-resolved magnetic structures in thin film and multilayer magnetic systems. The general advantage of the time-of-flight mode of operation over monochromatic instruments is a decoupling of spectral shape and polarization of the neutron beam with variable resolution. Thus, a wide Q-range can be investigated using a single angle of incidence, with resolution and flux well-adjusted to the experimental requirement. Our paper reviews the current status of the polarization equipment of the ToF reflectometer PLATYPUS and presents first results obtained on stratified Ni80Fe20/α-Fe2O3 films, revealing the distribution of magnetic moments in an exchange bias system. An outlook on the future development of the PLATYPUS polarization system towards the implementation of a polarized 3He cell is presented and discussed with respect to the efficiency and high Q-coverage up to 1 Å−1 and 0.15 Å−1 in the vertical and lateral momentum transfer, respectively.

Keywords

time, future, flight, neutron, developments, reflectometry, platypus, status, oolarized

Disciplines

Engineering | Physical Sciences and Mathematics

Publication Details

Authors

T Saerbeck, D L. Cortie, S Bruck, J Bertinshaw, S A. Holt, A Nelson, M James, W T. Lee, and F Klose

PNCMI 2012 - Polarized Neutrons for Condensed Matter Investigations 2012

Time-of-Flight Polarized Neutron Reflectometry on PLATYPUS: Status and Future Developments

T. Saerbeck[a,b,*], D. L. Cortie[a,c], S. Brück[a,d], J. Bertinshaw[a,d], S. A. Holt[a], A. Nelson[a], M. James[a,e], W. T. Lee[a], F. Klose[a]

[a]*Australian Nuclear Science and Technology Organisation, Menai, NSW, 2234, Australia*
[b]*University of Western Australia, School of Physics, 35 Stirling Highway, Crawley, WA 6009, Australia*
[c]*Institute for Superconducting and Electronic Materials, University of Wollongong, Wollongong, NSW, 2522, Australia*
[d]*School of Physics, University of New South Wales, Sydney, NSW, 2052, Australia*
[e]*Australian Synchrotron, 800 Blackburn Road, Clayton Vic 3168, Australia.*

Abstract

Time-of-flight (ToF) polarized neutron reflectometry enables the detailed investigation of depth-resolved magnetic structures in thin film and multilayer magnetic systems. The general advantage of the time-of-flight mode of operation over monochromatic instruments is a decoupling of spectral shape and polarization of the neutron beam with variable resolution. Thus, a wide Q-range can be investigated using a single angle of incidence, with resolution and flux well-adjusted to the experimental requirement. Our paper reviews the current status of the polarization equipment of the ToF reflectometer PLATYPUS and presents first results obtained on stratified $Ni_{80}Fe_{20}/\alpha$-Fe_2O_3 films, revealing the distribution of magnetic moments in an exchange bias system. An outlook on the future development of the PLATYPUS polarization system towards the implementation of a polarized ^{3}He cell is presented and discussed with respect to the efficiency and high Q-coverage up to $1\,\text{Å}^{-1}$ and $0.15\,\text{Å}^{-1}$ in the vertical and lateral momentum transfer, respectively.

Keywords: Polarized Neutron Reflectometry, Thin Film Magnetism, Time-of-Flight,

1. Introduction

   The research of magnetism in thin films and multilayers relies on experimental techniques with high sensitivity not only with respect to the magnetic moment, but also spatially across the film structure and internal boundaries. A prominent example for such a technique is polarized neutron reflectometry (PNR) [1], utilizing the dipole interaction of the neutron magnetic moment and the magnetic induction of the film. The technique reveals the spatially-resolved chemical and magnetic scattering length density (SLD) profiles along the normal and lateral directions of the thin film structure by measuring the spin-dependent scattered neutron intensity as a function of the momentum transfer $\boldsymbol{Q}$. In

---

* Corresponding author
   Email address: `tsaerbeck@physics.ucsd.edu` (T. Saerbeck)

typical PNR experiments, with collimation of the neutron beam only provided with respect to the incident angle α_i, the momentum transfer can be categorized into specular reflectivity, with

$$Q_Z = \frac{2\pi}{\lambda}[\sin(\alpha_i) + \sin(\alpha_f)] \,, \tag{1}$$

and off-specular or diffuse scattering, with

$$Q_X = \frac{2\pi}{\lambda}[\cos(\alpha_f) - \cos(\alpha_i)] \,, \tag{2}$$

where α_i and α_f are the incident and scattered angles of the neutron beam and λ the neutron wavelength. Specular reflected intensities contain the depth-resolved structural and magnetic information of the sample, while lateral periodicities manifest in off-specular scattering. While PNR is historically mostly residing in areas of hard-condensed matter research [2, 3], new soft-condensed matter applications are advancing. Experiments investigating the density profile of self-assembled monolayers and bilayers associated with biological membranes [4, 5, 6] and DNA biosensing systems [7] can make use of an additional contrast provided by a magnetic reference layer. In order to accommodate for the large area of applicability, the instrumental design needs to be flexible with respect to the scientific question, sample structure, sample environment and detection modes. In our paper, we review the current status and future development of the polarized neutron reflectometer PLATYPUS at the Bragg Institute, which is open to accept proposals using polarized neutrons [8].

Experimentally, the momentum transfer can be varied by means of changing the angle of incidence in a monochromatic, angle-dispersive reflectometer, or by the time-of-flight method, which is the mode of operation employed in PLATYPUS. Angle-dispersive reflectometer, such as NREX[+] at FRM2 [9], NG1 (now PBR) at NIST [10] and ADAM at ILL [11], operate with a fixed neutron wavelength and subsequently fixed wavelength resolution on the order of $\Delta\lambda/\lambda \approx 1.5\,\%$. In contrast, PLATYPUS provides a selectable wavelength resolution of $\Delta\lambda/\lambda = 1.3\,\%$, $\Delta\lambda/\lambda = 4.3\,\%$ and $\Delta\lambda/\lambda = 9\,\%$ by selecting disc chopper pairs at different distances [12]. This wavelength resolution range is comparable with other ToF instruments, for example D17 and FIGARO at the ILL [14, 13], POLREF at ISIS [15] and REFSANS at FRM2 [16]. The benefit of the selectable experimental resolution is a gain of 7× increased neutron flux for the low-resolution mode over the major part of the wavelength band [12]. A major advantage of the time-of-flight mode of operation due to the individual adjustable wavelength and angular resolution is the possibility to maintain a constant resolution $\Delta Q/Q$ and a spectral shape independent of the wavelength resolution. The timing signal of the disc-chopper can further be effectively used to stream each neutron scattering event, providing the time resolution of experiments investigating dynamical processes. The instrument is designed with a vertical scattering plane, allowing the investigation of solid thin-films, solid-liquid interfaces and free liquid surfaces. This high flexibility is one of the main characteristics of PLATYPUS and not constrained by the implementation of the PLATYPUS polarization system, providing efficiencies as high as 99.3 % over a large wavelength band [18].

2. Current Status

In the current setup, PLATYPUS allows for neutron beam polarization and spin-analysis of specular reflected intensities by using $m = 3.8$ polarizing Fe/Si supermirrors (SM) (Fig. 1). The reflective coating is provided on both top and bottom surfaces, resulting in a polarization efficiency as high as 99.3 % in a broad wavelength spectrum of $2.5\,\text{Å} < \lambda < 12.5\,\text{Å}$ at an incident angle of 0.8° on the SM. The broad wavelength bandwidth is essential for studies of dynamic systems in which the reflectivity changes as a function of time [12] and therefore requires the monitoring of a broad range of Q_Z-range simultaneously. Unlike the polarizer, whose axis is fixed with respect to the neutron beam, the analyzer SM tilt can be adjusted within ±14° and is mounted inside the evacuated detector tank on a vertical translation stage, allowing it to follow the specular reflection from the sample to scattering angles of 7° (Fig. 1). Over the flight path through the instrument, the neutron beam can be shaped with four horizontally and vertically adjustable slits. A slit package prior to the four disc-chopper system is used to adjust the total incoming intensity delivered into the instrument. The collimation of the neutron beam is regulated with two slit packages positioned in a distance of ~2835 mm, allowing to shape a neutron beam with a maximum area of 30 mm in height and 54 mm in width.

While the polarizer and analyzer SM can accommodate a 70 mm wide neutron beam, the vertical height is limited to a maximum of 7 mm at an angle of incidence of 0.8° due to the limited length of the SM. The analyzing SM has the same length, but is wider (104 mm) in order to account for the horizontal divergence of the neutron beam. Following the sample stage, the background can be suppressed with the fourth adjustable slit package on a vertical translation stage. Along the flight path, the neutron spin is maintained with an adjustable magnetic guide field provided by two solenoids before and after the sample stage. While this guide field constitutes the low-field option with minimum fields of 0.5 mT, the longitudinal orientation couples directly to the field provided at the sample stage, for example by the 1 T Bruker electromagnet (to a maximum 1 T in the 5-350 K cryogenic environment and 2.2 T without sample environment), enabling both positive and negative fields to be applied without any loss of polarization. With respect to this external field, the neutron spin can be inverted by two radio frequency (RF) spin flippers, mounted together with the SM in a compact magnetically shielded housing.

The commissioning of the polarization equipment revealed high efficiencies of the SM over the whole wavelength spectrum with a maximum of 99.3 % [18]. Flipping efficiencies of 99.7 % are achieved independent of the neutron wavelength by careful adjustment of the RF frequency and coil current magnitude. In operation with polarized neutrons, the rotation frequency of the choppers is increased from the typical 20 Hz to 33 Hz, adjusting the wavelength spectrum to the transmitted spectrum through the supermirror and further increasing the count rate by a factor of 1.6.

3. First Results

Polarized neutron reflectometry is a useful tool to study the magnetic reversal mechanism in nanomagnetic thin films, as it is able to differentiate between domain-wall motion and coherent rotation of ferromagnetic spins [20, 21, 22]. This technique has been used to directly reveal the different reversal mechanisms for a number of exchange-biased ferromagnetic/antiferromagnetic bilayers, providing a useful way to classify these systems [22, 21, 23] and to infer information about the antiferromagnetic interface behavior [24]. Using PLATYPUS, we investigated the reversal mechanism for a $Ni_{80}Fe_{20}$ (13.1 nm)/ α-Fe_2O_3 (14.5 nm) bilayer [25]. Fig. 2 shows the polarized neutron reflectometry pattern obtained for the sample at 45 K in a 20 mT applied field, where the permalloy is in the magnetically saturated state, evident in a large spin asymmetry between the R^{++} and R^{--} channels. The solid lines are the results of a quantitative fit to the experimental data that reveals that the permalloy layer has a magnetic moment of $0.96 \mu_B$ per atom, and no magnetic signal is present in the bulk part of the antiferromagnetic hematite layer. The fitted nuclear scattering density for hematite and permalloy, and their magnetic moments, are consistent with the respective bulk values and the profile suggested by the X-ray reflectometry investigation [25]. Near saturation, as shown in Fig. 2, the intensity measured in the spin-flip channel R^{+-} is low – near the level of experimental uncertainty, once the data has been corrected to take account of finite efficiency of the polarizing super-mirrors and spin-flippers. However, the
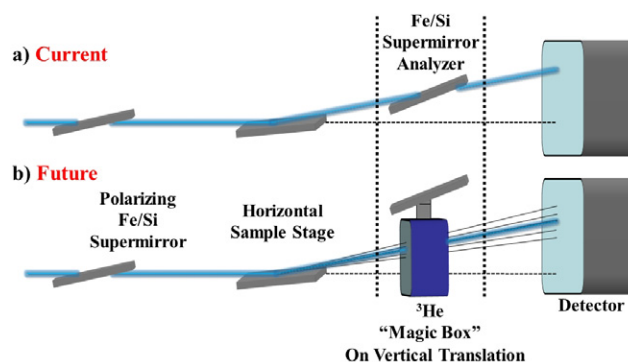

Fig. 1. (Color online) Current and future outline of the polarization setup on the ToF reflectometer PLATYPUS. The top schematic shows the utilization of two m=3.8 Fe/Si supermirrors to achieve neutron polarization and analysis of specular reflections (for explanation see text). The lower panel shows the envisaged implementation of a ^{3}He "magic box" on PLATYPUS, enabling the spin-dependent detection of off-specular scattering signals.
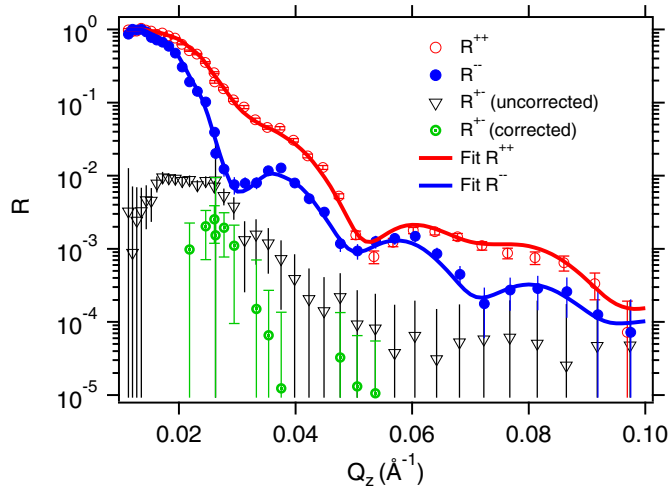
Fig. 2. $Ni_{80}Fe_{20}/\alpha$-Fe_2O_3 bilayer measured at 20 mT at 45 K in a saturated state corresponding to $0.96\,\mu_B$ per permalloy atom. After polarization correction, the spin-flip channel is reduced to the level of experimental uncertainty.
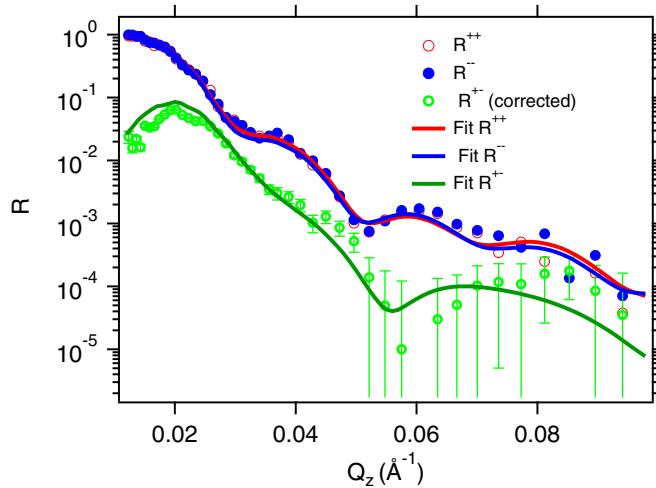

Fig. 3. $Ni_{80}Fe_{20}/\alpha$-Fe_2O_3 bilayer measured at - 14 mT at 5 K in the exchange bias state. The nearly zero spin asymmetry proves that this is measured near a coercive field. The large spin-flip signal is consistent with a transverse magnetic component associated with domain rotation and a low dispersion of magnetization-angles.

case is notably different for the sample in the field-cooled state at 5 K, when measured at -14.2 mT at a coercive field corresponding to an intermediate state of partial magnetic reversal. Fig. 3 shows the spin-flip and non-spin flip reflectivity patterns for the sample under these conditions. The similarity between the R^{++} and R^{--} patterns results in near-zero spin asymmetry. This is to be expected at a coercive field since, as by definition, the net magnetization along the field direction is zero at this point of the magnetic hysteresis loop. However, concurrently with the vanishing spin asymmetry, a large neutron spin-flip intensity is recorded in the R^{+-} channel, consistent with a component of magnetization in the permalloy layer that is rotated to $\approx 90°$ with respect to the applied field in the traverse in-plane direction. As in other exchange-bias systems such as Co/CoO [21], this large transverse magnetic component is associated with domain rotation in the applied field, and the magnitude of the spin-flip intensity can be directly related to the dispersion of ferromagnetic domain-angles [20]. In this case we find a low dispersion of angles, corresponding to a highly coherent magnetic reversal evident in $0.9\,\mu_B$ of the effective permalloy moment rotated to $\approx 90°$. Conversely,

if magnetic reversal were to occur by the motion or nucleation of domain structures that were exclusively co-axial with the applied field, no neutron spin-flip signal would be detected. In particular, for the $Ni_{80}Fe_{20}$ (13.1 nm)/ α-Fe_2O_3 (14.5 nm) bilayer it is found that the precise magnetic reversal mechanism depends on the degree of magnetic training, and is closely correlated with the macroscopic magnetic hysteresis loop determined by conventional SQUID magnetometry [25].

4. Future Developments

An upgrade of the instrument, currently in the commissioning phase, includes a spin polarization analysis via a ^{3}He "magic box" [19]. The ^{3}He-cell will accompany the existing setup without limiting the operation of the existing analyzer SM. The cell is included in a compact magnetic shielding box, mounted on the vertical translation stage below the analyzer SM. Thus, the two spin analyzing devices can easily be exchanged without interfering with the instrumental setup. Tests of the ^{3}He cell in the magnetostatic cavity of the Platypus analyser showed a polarisation lifetime of 200h. The polarising station polarises ^{3}He gas with polarisation in the analyser cell reaching 72 %. Once below the desired efficiency, the cell can be refreshed through the vacuum ports without breaking the vacuum of the detector tank. The main ^{3}He refurbishment station is outsourced with respect to the instrument and envisaged to serve for every instrument located at the Bragg Institute that operates polarized neutrons.

References

[1] C. H. Marrows, L. C. Chapon and S. Langridge, Materials Today 12 (7-8), 70-77 (2009).
[2] M.R. Fitzsimmons, S.D. Bader, J.A. Borchers, G.P. Felcher, J.K. Furdyna, A. Hoffmann, J.B. Kortright, I.K. Schuller, T.C. Schulthess, S.K. Sinha, M.F. Toney, D. Weller and S. Wolf Journal of Magnetism and Magnetic Materials **271**, 103 (2004).
[3] H. Zabel, Materials Today 9 (1-2), 42 (2006).
[4] S.A. Holt, A.P. Le Brun, C.F. Majkrzak, D.J. McGillivray, F. Heinrich, M. Losche and J.H. Lakey, Soft Matter **5**, 2576 (2009).
[5] A.P. Le Brun, S.A. Holt, D.S.H. Shah, C.F. Majkrzak and J.H. Lakey, Biomaterials **32**, 3303 (2011).
[6] A.P. Le Brun, S.A. Holt, D.S. Shah, C.F. Majkrzak, J.H. Lakey, European Biophysics Journal with Biophysics Letters **37**, 639 (2008).
[7] T.H.M. Kjällman, A.R.J. Nelson, M. James, J.A. Dura, J. Travas-Sejdic and D.J. McGillivray, Soft Matter **7**, 5020 (2011).
[8] The Bragg Institute Neutron Beam Instrument proposal system is available at https://neutron.ansto.gov.au
[9] http://www.frm2.tum.de/wissenschaftliche-nutzung/diffraktion/n-rex/index.html
[10] http://www.ncnr.nist.gov/instruments/ng1refl/
[11] http://www.ill.eu/instruments-support/instruments-groups/instruments/superadam/
[12] M. James, A. Nelson, S. A. Holt, T. Saerbeck, W. A. Hamilton and F. Klose, Nuclear Instruments and Methods in Physics Research Section A: Accelerators, Spectrometers, Detectors and Associated Equipment **632**, 112 (2011).
[13] R. A. Campbell, H. P. Wacklin, I. Sutton, R. Cubitt and G. Fragneto, The European Physical Journal Plus **126**, 1 (2011).
[14] R. Cubitt and G. Fragneto, Applied Physics A, s329-s331 (2002).
[15] http://www.isis.stfc.ac.uk/instruments/polref/technical/polref-technical-information7280.html
[16] R. Kampmann, M. Haese-Seiller, V. Kudryashov, V. Deriglazov, V. Syromiatnikov, M. Tristl, B. Toperverg, A. Okorokov, A. Schreyer and E. Sackmann, Physica B: Condensed Matter **335**, 274 (2003).
[17] M. James, A. Nelson, A. Brule and J. C. Schulz, Journal of Neutron Research **14(2)**, 91-108 (2006).
[18] T. Saerbeck, F. Klose, A. P. L. Brun, J. Füzi, A. Brule, A. Nelson, S. A. Holt and M. James, Review of Scientific Instruments, **83**, 081301 (2012).
[19] Designed by one of the authors and manufactured at the Institut Laue Langevin (ILL).
[20] W.-T. Lee, S. G. E. te Velthuis, G. P. Felcher, F. Klose, T. Gredig, and E. D. Dahlberg, Phys. Rev. B. **65**, 224417(2002).
[21] M. Gierlings, M. J. Prandolini, H. Fritzsche, M. Gruyters, and D. Riegel, Phys. Rev. B **65**, 092407 (2002).
[22] M. R. Fitzsimmons, P. Yashar, C. Leighton, I. K. Schuller, J. Nogués, C. F. Majkrzak, and J. A. Dura, Phys.Rev. Lett. **84**, 3986 (2000).
[23] P. Blomqvist, K. M. Krishnan, and H. Ohldag, Phys. Rev. Letters **94**, 107203 (2005).
[24] A. Hoffmann, Phys. Rev. Lett. **93**, 097203 (2004).
[25] D. L. Cortie, K.W. Lin, C. Shueh, H. F. Hsu, X. L. Wang, M. James, H. Fritzsche, S. Brück, and F. Klose, Phys. Rev. B **86**, 054408 (2012).